

EUROSENSORS 2015

# Electrical conductivity and gas-sensing properties of Mg-doped and undoped single-crystalline $\text{In}_2\text{O}_3$ thin films: bulk vs. surface

J. Rombach<sup>a,\*</sup>, O. Bierwagen<sup>a</sup>, A. Papadogianni<sup>a</sup>, M. Mischo<sup>b</sup>, V. Cimalla<sup>b</sup>, T. Berthold<sup>c</sup>,  
S. Krischok<sup>c</sup>, M. Himmerlich<sup>c</sup>

<sup>a</sup>Paul-Drude-Institut für Festkörperelektronik, Berlin, Germany

<sup>b</sup>Fraunhofer Institut für Angewandte Festkörperphysik, Freiburg, Germany

<sup>c</sup>Institut für Physik and Institut für Mikro- und Nanotechnologien, Technische Universität Ilmenau, Germany

## Abstract

This study aims to provide a better fundamental understanding of the gas-sensing mechanism of  $\text{In}_2\text{O}_3$ -based conductometric gas sensors. In contrast to typically used polycrystalline films, we study single crystalline  $\text{In}_2\text{O}_3$  thin films grown by molecular beam epitaxy (MBE) as a model system with reduced complexity. Electrical conductance of these films essentially consists of two parallel contributions: the bulk of the film and the surface electron accumulation layer (SEAL). Both these contributions are varied to understand their effect on the sensor response. Conductance changes induced by UV illumination in air, which forces desorption of oxygen adatoms on the surface, give a measure of the sensor response and show that the sensor effect is only due to the SEAL contribution to overall conductance. Therefore, a strong sensitivity increase can be expected by reducing or eliminating the bulk conductivity in single crystalline films or the intra-grain conductivity in polycrystalline films. Gas-response measurements in ozone atmosphere test this approach for the real application.

© 2015 The Authors. Published by Elsevier Ltd. This is an open access article under the CC BY-NC-ND license (<http://creativecommons.org/licenses/by-nc-nd/4.0/>).

Peer-review under responsibility of the organizing committee of EUROSENSORS 2015

**Keywords:** Conductometric gas sensors, MBE, single crystalline, doping, Indium oxide, Ozone sensors

## 1. Introduction

Indium oxide is a well-known material for conductometric gas sensors, showing a change in conductance when exposed to oxidizing gases such as ozone [1]. Particularly attractive is the possibility to reactivate the sensor surface

\* Corresponding author. Tel.: +49.30.20377.268; fax: +49.30.20377.201.

E-mail address: [rombach@pdi-berlin.de](mailto:rombach@pdi-berlin.de)

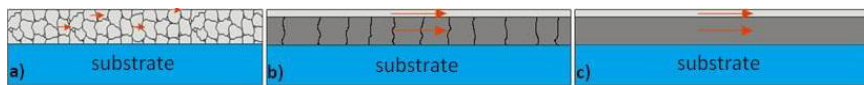


Fig. 1: Sketches of: a) a polycrystalline film, b) a textured film and c) a single-crystalline film.

by UV-induced photoreduction of the surface [2], enabling gas sensor operation at room temperature. For polycrystalline layers it has been shown that a thin surface-near layer has the major contribution to the gas sensitivity [1]. The  $\text{In}_2\text{O}_3$  films possess a surface electron accumulation layer (SEAL) that governs the surface conductance and can be removed by oxygen plasma treatment of the surface [3]. A study on the correlation of these two surface phenomena and a detailed understanding of the underlying mechanisms, however, are difficult due to the complex electron transport path in the typically used polycrystalline material (see arrows in Fig 1 a) with contributions from the bulk of the grains, the surface, and across and along grain boundaries. With a semiconductor-science view on  $\text{In}_2\text{O}_3$  [3] we aim to get a better understanding of the gas-sensing mechanism using MBE-grown single-crystalline  $\text{In}_2\text{O}_3$  thin films on insulating Y-stabilized  $\text{ZrO}_2$  (YSZ) substrates with only two electrically parallel contributions to their total conductance, bulk and surface (Fig 1 c), as well as textured films on  $\text{Al}_2\text{O}_3$  substrates consisting of single-crystalline rotational domains (Fig 1b) with three conductance contributions: bulk, surface and across domain boundaries. By thickness reduction,  $\text{O}_2$ -annealing (reducing the number of the donor oxygen vacancies) or Mg-doping (as compensating deep acceptors) [3], the bulk contribution to the overall conductance was systematically decreased.

## 2. Experimental

Our films were grown by plasma-assisted MBE under oxygen-rich conditions on (111) oriented YSZ and (0001) oriented  $\text{Al}_2\text{O}_3$  substrates at substrate temperatures of 750-800°C, measured by a pyrometer. In-situ reflection high-energy diffraction (RHEED) and laser reflectometry were used to monitor surface morphology and growth-rate, respectively. X-ray diffraction (XRD) and atomic force microscopy were used for structural characterization of the samples. Further treatment was done by rapid thermal annealing in  $\text{O}_2$  for 60 s at 800 °C and by oxygen-plasma treatment with a reactive ion-etching system using a plasma power of 50 W. X-ray photoelectron spectroscopy (XPS) measurements were performed using monochromated  $\text{AlK}\alpha$  radiation ( $h\nu = 1486.7$  eV) in normal emission. Four point-probe sheet conductance measurements using the van der Pauw method in air were performed under UV-illumination by a light-emitting diode (LED) with a peak wavelength of 400 nm, energetically below the optical bandgap of  $\text{In}_2\text{O}_3$  [2, 3]. UV-illumination forces desorption of adsorbed oxygen species leading to an increase of conductance, which yields a measure of the response to oxidizing gases such as  $\text{O}_3$ . Finally, gas-response measurements in a controlled atmosphere of synthetic air and  $\text{O}_3$  were done to confirm our results.

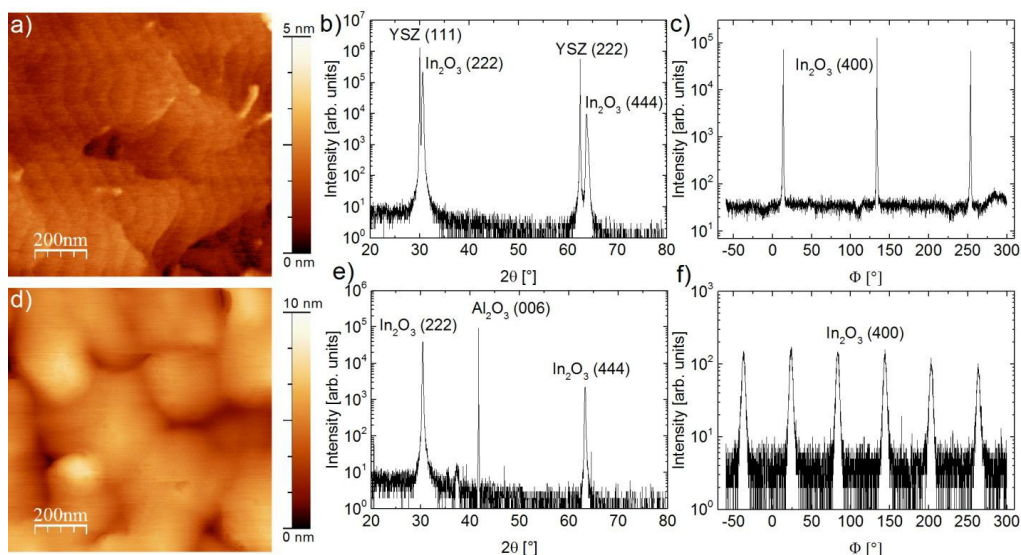


Fig. 2: AFM images and XRD ( $2\theta$ - $\omega$ ) and  $\Phi$  scans) of films on YSZ (a, b, c) and  $\text{Al}_2\text{O}_3$  (d, e, f).

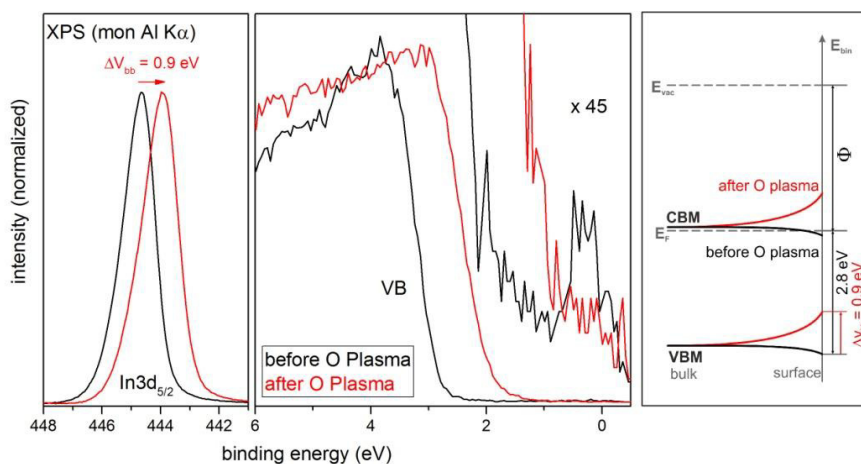


Fig. 3: XPS spectra and resulting surface band bending of an as grown and an oxygen plasma-treated  $\text{In}_2\text{O}_3$  film.

### 3. Results

Fig. 2 b,c) shows XRD  $2\theta$ - $\omega$  and  $\Phi$  scans of the film on YSZ confirming that the film exhibits only the (111) out-of-plane orientation and one in-plane orientation (three peaks in the  $\Phi$  scan due to the three-fold symmetry of the (111) surface), confirming its single-crystallinity. Fig. 2 e) and f) also confirm the (111) out-of-plane orientation of the film on  $\text{Al}_2\text{O}_3$  and the presence of two in-plane orientations (rotational domains) due to six peaks in the  $\Phi$  scan. Fig. 2 a) and d) show AFM images of films on YSZ and  $\text{Al}_2\text{O}_3$  with RMS surface roughnesses of 0.5 nm and 1.2 nm, respectively. Domains of the textured film are visible Fig. 2 d) and flat terraces with atomic steps of the single-crystalline film in Fig. 2 c).

XPS confirmed the existence of the SEAL on the as grown (Fig. 3) and  $\text{O}_2$ -annealed  $\text{In}_2\text{O}_3$  films (not shown). The spectra of an as grown and a plasma treated sample in Fig. 3 show a shift of valence band and core-levels towards the Fermi level and a reduction of the SEAL peak (45x magnified view), indicating a near-surface upward band-bending and depletion of the SEAL after plasma-treatment.

To study the gas-response of our films, the absolute and relative changes in sheet conductance  $\Delta G = G_{\text{max}} - G_{\text{min}}$ , and  $\text{SENS} = G_{\text{max}}/G_{\text{min}}$ , upon UV-illumination in air are compared. Fig. 4 a) shows measurements of sheet conductance over time of three undoped textured films, as grown,  $\text{O}_2$ -annealed, oxygen plasma-treated and one  $\text{O}_2$ -annealed single-crystalline film. The UV-LED was switched on and off repeatedly every 120 s until  $\Delta G$  remained constant, the previous cycles were not used for further analysis. Comparing the as grown and the  $\text{O}_2$ -annealed textured films, we find that both  $\Delta G$  and  $\text{SENS}$  are higher for the  $\text{O}_2$ -annealed film and  $\tau_{\text{off}}$ , extracted from exponential fits of the UV-off data in order to get a measure of the response times of the films, is higher for the as grown film. The higher  $\text{SENS}$  value of the  $\text{O}_2$ -annealed film can be caused by the lower response time or by the decrease of bulk conductivity after  $\text{O}_2$ -annealing. To disentangle these effects,  $\Delta G$  and  $\text{SENS}$  were measured in equilibrium-states (Fig. 4 b and c). The different response times will be studied separately. The undoped reference in Fig. 4 b) shows a similar  $\Delta G$  for as grown and  $\text{O}_2$ -annealed films but higher  $\text{SENS}$  for the  $\text{O}_2$ -annealed film. This confirms that for the non-equilibrium case (Fig. 4a), the lower  $\Delta G$  of the as grown film is due to its higher response time and the higher  $\text{SENS}$  value of the  $\text{O}_2$  annealed film is due to both faster response and lower bulk conductivity. In the equilibrium case (Fig. 4 b), the higher  $\text{SENS}$  value of the  $\text{O}_2$  annealed film is only due to the lower bulk conductivity. Hence the change in conductance upon UV-induced O-desorption is mainly occurring in the SEAL. This is further confirmed by the fact that both  $\Delta G$  and  $\text{SENS}$  decrease drastically after oxygen-plasma treatment, depleting the SEAL. Comparing textured and single-crystalline films, we find that  $\Delta G$  and  $\text{SENS}$  are similar but  $\tau_{\text{off}}$  is slightly higher for the textured film, possibly due to domain-boundary effects.

To increase the gas-response of our films, the bulk contribution to overall conductance was further decreased by Mg-doping or thickness reduction (Fig. 4 b and c), comparing  $\Delta G$  and  $\text{SENS}$  in equilibrium-states ( $G_{\text{max}}$ : LED on until  $G$  remains constant,  $G_{\text{min}}$ : after storing the samples in the dark for several hours). Fig. 4 b) shows that  $\Delta G$  remains roughly constant up to a medium Mg-concentration ( $N_{\text{Mg}}$ ), including the undoped reference. Due to the decrease of the bulk conductance with higher  $N_{\text{Mg}}$ ,  $\text{SENS}$  increases by roughly one order of magnitude.  $G_{\text{min}}$  is  $2.2 \times 10^{-4}$  S,  $1.0 \times 10^{-5}$  S and  $1.1 \times 10^{-6}$  S for the  $\text{O}_2$ -annealed Mg-doped films with  $N_{\text{Mg}}$  of  $10^{18}$   $\text{cm}^{-3}$ ,  $10^{19}$   $\text{cm}^{-3}$  and

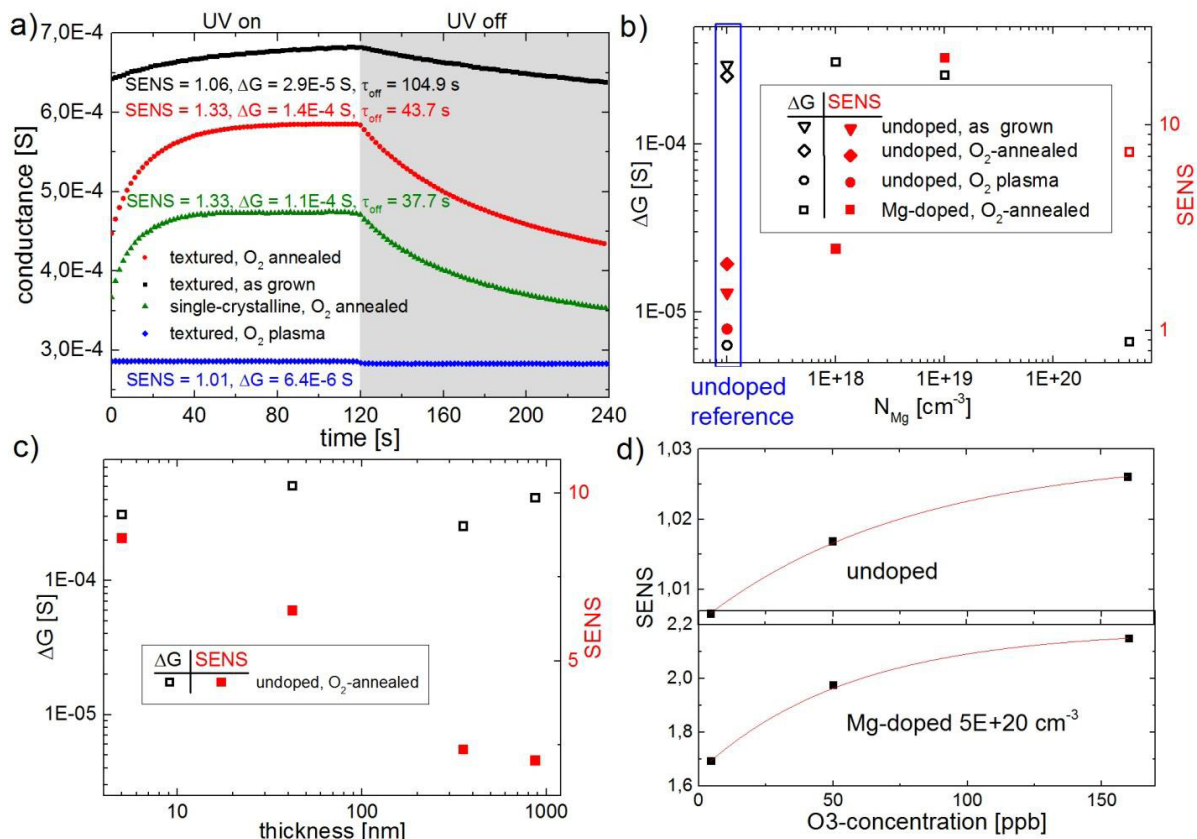


Fig 4: Gas-response measurements in air of undoped single-crystalline and textured films which have undergone different post-growth treatments (a), Mg-doped textured films with different Mg-concentrations (b) and undoped single-crystalline films of different thicknesses, all O<sub>2</sub>-annealed (c). Graph d) shows gas-response measurements in O<sub>3</sub>-atmosphere of undoped and Mg-doped O<sub>2</sub>-annealed textured films.

$5 \times 10^{20} \text{ cm}^{-3}$ , respectively. For high  $N_{Mg}$  however,  $\Delta G$  and SENS decrease, likely due to a depletion of the SEAL by the high concentration of compensating acceptors exceeding the electron concentration of the SEAL. Fig. 4 c) shows the dependence of  $\Delta G$  and SENS on the film thickness for undoped, single crystalline films.  $\Delta G$  is roughly constant for film thickness changes of almost two orders of magnitudes and as expected, SENS increases for decreasing film thicknesses due to the decreasing bulk contribution.

Fig. 4 d) shows gas-response measurements in an atmosphere of synthetic air and varying O<sub>3</sub>-concentration of undoped and a Mg-doped film, both textured. Similar as in the measurements in air, the sensitivity to O<sub>3</sub> increases strongly with Mg-doping. However, both films are sensitive enough to resolve O<sub>3</sub>-concentrations as low as 50 ppb.

In conclusion, our results show that the gas-response of single crystalline or textured In<sub>2</sub>O<sub>3</sub> thin films is exclusively due to a change of the SEAL contribution to the overall conductance of the film. By reducing the electrically parallel bulk conductance, e.g. by Mg doping, a significant sensitivity increase can be realized. In addition to serving as a model system, our single crystalline films sense gases effectively and may offer benefits due to the absence of grain boundaries.

**Acknowledgement:** This work was supported by the DFG grants AM105/31-1, BI 1754/1-1, and HI 1800/1-1.

#### References

- [1] G. Kiriakidis et al. (2001): Ozone Sensing Properties of Polycrystalline Indium Oxide Films at Room Temperature. *phys. Stat. sol. A* **185**, 27-32.
- [2] Ch. Y. Wang et al. (2011): Photon stimulated sensor based on indium oxide nanoparticles I: Wide-concentration-range ozone monitoring in air. *Sens. Actuators B* **152**, 235.
- [3] O. Bierwagen (2015): Indium oxide—a transparent, wide-band gap semiconductor for (opto)electronic applications, *Semicond. Sci. Technol.* **30**, 024001.